Effects of Photosensitizers and Reaction Media on Light-Driven Water Oxidation with Trinuclear Ruthenium Macrocycles

Ana-Lucia Meza-Chincha,[a] Dorothee Schindler,[a] Mirco Natali,[b] and Frank Würthner*[a, c]

Photocatalytic water oxidation is a promising process for the production of solar fuels and the elucidation of factors that influence this process is of high significance. Thus, we have studied in detail light-driven water oxidation with a trinuclear Ru(bda) (bda: 2,2′-**bi**pyridine-6,6′-**di**carboxylate) macrocycle **MC3** and its highly water soluble derivative ***m*-CH_2NMe_2-MC3** using a series of ruthenium tris(bipyridine) complexes as photosensitizers under varied reaction conditions. Our investigations showed that the catalytic activities of these Ru macrocycles are significantly affected by the choice of photosensitizer (PS) and reaction media, in addition to buffer concentration, light intensity and concentration of the sensitizer. Our steady-state and transient spectroscopic studies revealed that the photocatalytic performance of trinuclear Ru(bda) macrocycles is not limited by their intrinsic catalytic activities but rather by the efficiency of photogeneration of oxidant PS^+ and its ability to act as an oxidizing agent to the catalysts as both are strongly dependent on the choice of photosensitizer and the amount of employed organic co-solvent.

1. Introduction

Artificial photosynthesis is an emerging technology for the generation of renewable and carbon-neutral energy as it allows the storage of solar energy in chemical bonds of "solar fuels" such as hydrogen or other compounds generated by the reduction of CO_2.[1] In this context, the oxidation of water to molecular oxygen is essential as it provides the reducing equivalents required.[2] Accordingly, the development of water oxidation catalysts (WOCs) has been a subject of intense research in the last decades.[3] Among numerous homogeneous catalysts based on Ru, Ir and first-row transition metals,[4] Ru(bda) WOCs[5] have attracted much attention as some of these catalysts reach catalytic activities comparable to those of the oxygen-evolving complex of photosystem II.[6]

The study of water oxidation by molecular catalysts can be accomplished by chemical, electrochemical and photochemical methods.[3] The latter method is of pivotal importance for the application of WOCs in solar fuels devices. As in natural photosynthesis, a key process in light-driven water oxidation is the activation of the WOC by oxidants generated by irradiation of a photosensitizer. Thus, the photocatalytic activities of homogeneous WOCs are generally studied by means of a three-component system comprising a photosensitizer (PS), a sacrificial electron acceptor and the catalyst. As shown in Figure 1, after activation of the PS to the excited state PS* by light [Eq. (1)], the oxidant PS^+ is produced by one-electron transfer from PS* to the electron acceptor [Eq. (2)] and PS is then regenerated by oxidation of the WOC [Eq. (5)]. Upon transfer of four electrons in a photocatalytic cycle, water is oxidized to molecular oxygen and four protons and four electrons are released [Eq. (6)].[7] Although several PS and electron acceptor systems have been applied in photocatalytic water oxidation,[8] ruthenium tris(bipyridine) as PS and sodium persulfate as electron acceptor have become a standard combination for light-driven water oxidation by homogeneous WOCs. On the one hand, ruthenium tris(bipyridine) complexes are excellent photosensitizers due to their good absorption of visible light, efficient generation of a long-lived triplet metal-to-ligand charge transfer (^{3}MLCT) state and relatively high oxidation potential of their oxidized form PS^+, which enables oxidation of WOCs to higher oxidation states.[9] On the other hand, the irreversible splitting of the persulfate ion upon one-electron reduction into a sulfate ion and a sulfate radical anion [Figure 1; Eq. (2)] limits competitive recombination processes which can reduce the efficiency of photocatalytic water oxidation.[10] In addition, the strong oxidant nature of the sulfate radical anion leads to the generation of a second equivalent of PS^+ from PS as indicated in [Eq. (3)].[10-,11] Accordingly, two PS molecules are oxidized by one persulfate ion upon light irradiation in a two-step process [Eq. (4)].[12] While the initial oxidation of the excited PS* takes place in the

[a] *A.-L. Meza-Chincha, D. Schindler, Prof. Dr. F. Würthner*
Institut für Organische Chemie
Universität Würzburg
Am Hubland, 97074 Würzburg (Germany)
E-mail: wuerthner@uni-wuerzburg.de
[b] *Prof. Dr. M. Natali*
Department of Chemical and Pharmaceutical Sciences
University of Ferrara
Via L. Borsari 46, 44121 Ferrara (Italy)
[c] *Prof. Dr. F. Würthner*
Center for Nanosystems Chemistry (CNC)
Universität Würzburg
Theodor-Boveri-Weg, 97074 Würzburg (Germany)

Supporting information for this article is available on the WWW under https://doi.org/10.1002/cptc.202000133

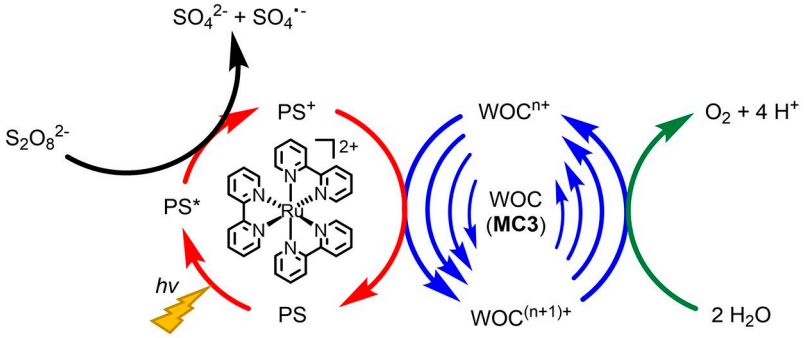

$$PS \xrightarrow{hv} PS^* \quad (1)$$

$$PS^* + S_2O_8^{2-} \longrightarrow PS^+ + SO_4^{2-} + SO_4^{\bullet-} \quad (2)$$

$$PS + SO_4^{\bullet-} \longrightarrow PS^+ + SO_4^{2-} \quad (3)$$

$$2\,PS + S_2O_8^{2-} \xrightarrow{hv} 2\,PS^+ + 2\,SO_4^{2-} \quad (4)$$

$$PS^+ + WOC^{n+} \longrightarrow PS + WOC^{(n+1)+} \quad (5)$$

$$2\,H_2O \xrightarrow{WOC^{(n+1)+}} O_2 + 4\,H^+ + 4\,e^- \quad (6)$$

Figure 1. Schematic illustration of the catalytic cycle of photocatalytic water oxidation using ruthenium tris(bipyridine) as PS, $Na_2S_2O_8$ as sacrificial electron acceptor and trinuclear Ru complexes (e.g. **MC3**) as WOC. The individual steps leading to oxidation of water are indicated in Equations (1–6).[3,18]

ns time regime, the dark thermal quenching by the sulfate radical is observed in the µs range.[13] Notably, light-driven water oxidation is a very complex process not only due to the involvement of the three essential components (WOC, PS and electron acceptor), but also due to the interplay of several additional factors that can drastically affect its efficiency as well. These include, e.g. light intensity,[13a,14] pH of the solution,[13b,15] chosen buffer system[13a,16] and its concentration.[16b,17]

We have previously reported that trinuclear Ru(bda) macrocycle **MC3** (Figure 2) is a highly efficient catalyst for chemical water oxidation using ceric ammonium nitrate (CAN) as an oxidant under acidic conditions.[19] Kinetic studies and ^{18}O labelling experiments have shown that this supramolecular WOC operates by a WNA mechanism (WNA: **w**ater **n**ucleophilic

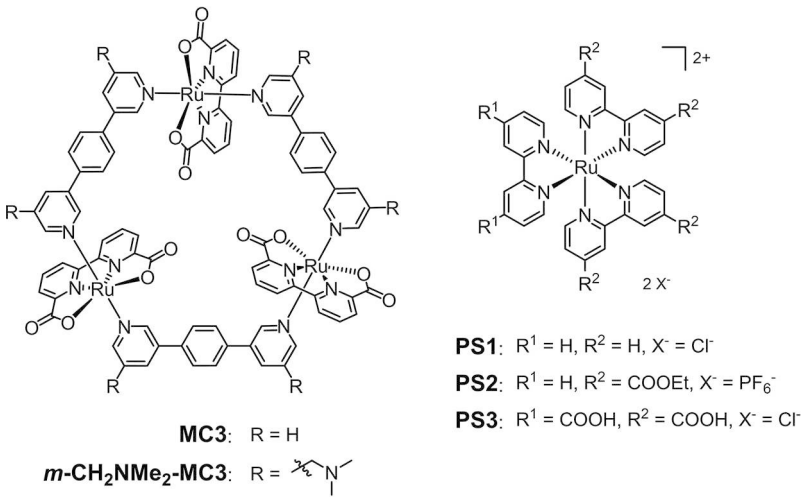

Figure 2. Chemical structures of Ru(bda) macrocycles **MC3** and ***m*-CH_2NMe_2-MC3** used in photocatalytic water oxidation and ruthenium tris(bipyridine) sensitizers **PS1–3**.

attack) as the O–O bond is formed by the attack of a water molecule on a $Ru^{V}=O$ intermediate.[19] Based on molecular dynamics simulations, we proposed the formation of a hydrogen-bonded network of water molecules inside the cavity of **MC3**[20] which might allow efficient proton transfer between the Ru centers following a Grotthuss-type mechanism.[21] Presumably, the preorganization of water molecules in the macrocyclic cavity reduces activation barriers for proton-coupled reaction steps resulting in the high catalytic activity of the WOC.

It has been reported in literature that catalytic performance (that means TOF and TON values) of homogeneous WOCs under light-driven conditions is typically inferior than under chemical or electrochemical conditions.[13b,14b] Indeed, this is also the case for trinuclear Ru(bda) macrocycle **MC3** and its derivatives.[19,22] This motivated us to address the unveiled question, why photocatalytic activities of Ru macrocycles are less efficient than those of chemical counterpart and which factors influence the photocatalytic activities of Ru(bda) macrocycles. Therefore, we have now explored the photocatalytic activities of **MC3** and its derivative ***m*-CH_2NMe_2-MC3**[23] as prime examples for the class of Ru(bda) macrocyclic WOCs under different reaction conditions using a series of ruthenium tris(bipyridine) derivatives **PS1-3**[24] as photosensitizers and sodium persulfate as electron acceptor (Figure 2). Macrocycle ***m*-CH_2NMe_2-MC3**, bearing six trialkylamine groups in axial ligands, was chosen as WOC to study the effect of the reaction media, particularly content of organic co-solvent, on the efficiency of photocatalysis as its solubility in water is significantly higher compared to parent **MC3**. Although, chemical water oxidation with this water-soluble derivative has been reported previously,[23] its photocatalytic activities under light-driven conditions remained unexplored. For these studies, the photosensitizer selection includes the standard, parent ruthenium tris(bipyridine) complex **PS1** and derivatives **PS2** and **PS3** bearing electron withdrawing groups to increase PS^{+}/PS oxidation potentials and thermodynamic driving force for activation of the WOC.[17a,c] The kinetic processes that determine the efficiency of photocatalysis were analyzed by steady-state and transient spectroscopic techniques. Here we report that the photocatalytic performances of Ru(bda) macrocycles are strongly dependent on the applied photosensitizer and reaction media, in particular, amount of organic co-solvent used. These findings are explained based on detailed analysis of steady-state emission quenching of photosensitizers and electron-transfer processes between sensitizer and WOC by nanosecond flash photolysis.

2. Results

2.1. Redox and Optical Properties

The redox properties of the Ru(bda) macrocycles **MC3** and ***m*-CH_2NMe_2-MC3** have been reported previously.[19–20,22–23] The electrochemical properties of the photosensitizers **PS1–3** were studied by cyclic voltammetry (CV) and differential pulse voltammetry (DPV) in phosphate buffered MeCN/H_2O (1:1, v/v) (Figure S1a) and pure water (Figure S2a) at pH 7. The redox and optical properties of the sensitizers are summarized in Table S1. A reversible $Ru^{III/II}$ oxidation process was observed for each of the sensitizers **PS1–3** in both solvents. Notably, the four electron withdrawing carboxylic ester groups of **PS2** imparted a significant increase in the $Ru^{III/II}$ oxidation potential of about 250 mV compared to parent compound **PS1** ($E_{PS1} = +1.39$ V *vs.* NHE) which complies with literature reported values.[16b,17a,c] The oxidation potential of **PS3** shows some dependency on the solvent composition since its value increased by 100 mV in the absence of organic co-solvent MeCN. This could be related to partly deprotonation of the carboxylic acid groups and kinetic barriers originating from the stronger hydrogen bonding in pure water as reported elsewhere.[25]

The optical properties of **PS1–3** were characterized by UV/Vis absorption and steady-state emission spectroscopy in phosphate buffered MeCN/H_2O 1:1 and pure water (pH 7, Table S1). For emission spectra, samples were degassed with argon to avoid quenching by oxygen. The absorption spectra of compounds **PS1–3** at room temperature show typical transitions characteristic of the ruthenium tris(bipyridine) moiety (Figures S1b and S2b).[26] These are: (i) a π-π^* bpy-ligand centered absorption band at around 300 nm, (ii) a Laporte forbidden metal centered d-d transition at about 350 nm and (iii) a broad ^{1}MLCT band at 450 nm. The electron withdrawing groups of **PS2** and **PS3** led to bathochromic shifts in MLCT absorption (30 nm and 13 nm, respectively) and emission (45 nm and 11 nm, respectively) compared to parent compound **PS1** in both solvents. Moreover, the absorption and emission maxima of the sensitizers are independent of the solvent composition. In contrast, the emission lifetime is affected by the used co-solvent as significantly higher lifetimes are observed in MeCN/H_2O 1:1 compared to those in pure water (Figure S3). For example, **PS2** showed a lifetime of 560 ns in buffered water, whereas in MeCN/H_2O 1:1 (pH 7) a significantly longer lifetime of 950 ns was observed. This solvent dependency could be explained based on preferential solvation of the sensitizers by the organic co-solvent in MeCN/H_2O mixtures.[12,27]

2.2. Photocatalytic Water Oxidation

We have explored first the effects of light intensity as well as concentration of buffer and photosensitizer on light-driven water oxidation by Ru(bda) macrocycle **MC3**. As a light source a xenon lamp was used ($\lambda = 400$–1000 nm, Figure S4) and the generated oxygen was detected with a Clark electrode (see SI for experimental details).

Using standard sensitizer **PS1** and sodium persulfate as sacrificial electron acceptor, the catalytic activity of macrocycle **MC3** was investigated in buffered MeCN/H_2O 1:1 (v/v, pH 7) at different phosphate buffer concentrations. As illustrated by the plot of the oxygen generation as a function of time (Figure 3a), under otherwise identical conditions (concentration of **PS1**, sodium persulfate and catalyst, light intensity and solvent composition), **MC3** performs around 25% higher TOF and TON

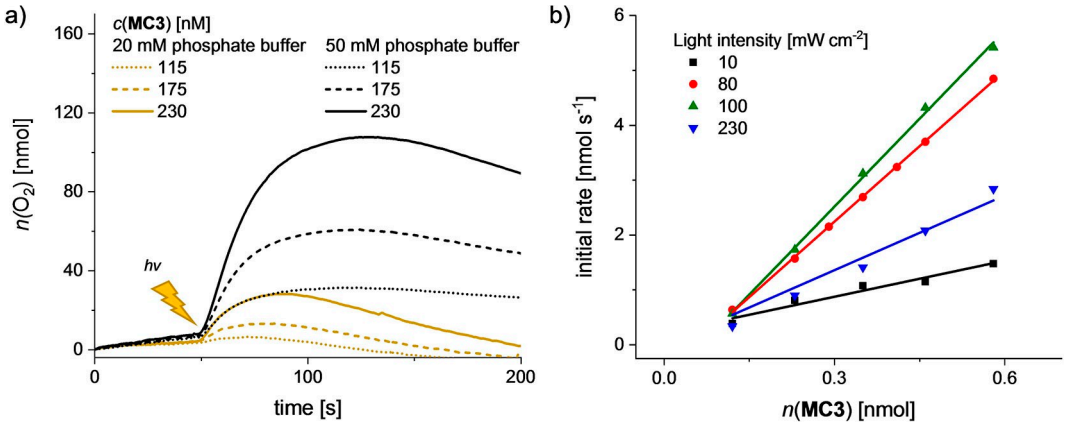

Figure 3. a) Catalyst concentration-dependent oxygen evolution curves of **MC3** in MeCN/H_2O 1:1 in 20 mM and 50 mM phosphate buffer solutions at pH 7, c(**PS1**) = 1.5 mM, $c(Na_2S_2O_8)$ = 37 mM, c(**MC3**) = 115–230 nM. The lighting symbol indicates the start of sample irradiation (light intensity: 100 mW cm^{-2}). b) Initial rates of oxygen generation by **MC3** at variable light intensities. Experiments were performed in MeCN/H_2O 1:1 (50 mM phosphate buffer, pH 7), c(**PS1**) = 1.5 mM, $c(Na_2S_2O_8)$ = 37 mM, c(**MC3**) = 60–290 nM.

values in 50 mM phosphate buffer compared to a more dilute 20 mM buffer solution (Table S2). While the pH at the end of catalysis remained constant in 50 mM phosphate buffer (pH 7), we observed a reduction down to pH 5.5 in the case of 20 mM solution. Accordingly, the higher catalytic activity at 50 mM buffer concentration can be ascribed to a stronger buffering effect. The higher amount of phosphate anions might also facilitate atom-proton transfers (APT)[28] leading to efficient formation of Ru^{III}-hydroperoxo intermediates as it has been described for mononuclear Ru(bda) complexes in electrochemical water oxidation.[29] Note that after reaching a plateau of maximal oxygen concentration, some of the dissolved oxygen is released into the gas phase which results in a decrease in the amount of gas detected by the Clark electrode.

As depicted in Figure 3b, the photocatalytic performance of WOC **MC3**, which is reflected in the initial rates of catalysis, is also strongly dependent on the light intensity used (Table S2, Figure S5). The highest TOF (10.9 s^{-1}) was obtained at 100 mW cm^{-2} (Table S2, entry 4), which is about the irradiance of the Sun at the Equator.[30] Decreasing light power down to 10 mW cm^{-2} led to a drastic loss in catalytic activity (TOF = 3.0 s^{-1}), presumably due to a slower activation of the sensitizer and corresponding photogeneration of PS^+.[31] Likewise, at a higher light power of 230 mW cm^{-2} TOF reduced to 5.3 s^{-1}. This might be reasoned by a more facile photodecomposition of the sensitizer under intense light exposure.[15a,32] Further, we investigated the effect of light intensity on quantum yields Φ and chemical yields of oxygen production ϕ_{chem} (Table S2, see SI for details). Our results indicate a correlation between the TONs and ϕ_{chem}, although for the latter due to the large excess of $Na_2S_2O_8$ (c = 37 mM) only values below 1% were obtained. At 10 mW cm^{-2} the highest Φ of 7.9% was observed, corresponding to an overall quantum efficiency (QE) of 15.8%.[8] At 100 mW cm^{-2} and 230 mW cm^{-2}, Φ decreased to 2.9% and 0.6%, respectively. These results comply well with recent observations that a careful adjustment of the photon flux is relevant towards the optimization of the light-driven catalytic response.[31,33] The concentration of photosensitizer affects the catalytic activity of **MC3** as well. Increasing the concentration of **PS1** from 0.2 mM to 1.5 mM resulted in a significant increase of TOF and TON values (Table S2, entries 4 and 6, Figure S6). Notably, no oxygen was produced in the absence of the WOC neither at 0.2 mM nor 1.5 mM concentration of **PS1** as revealed by control experiments (Figure S7). Likewise, no oxygen generation was detected in the absence of the sensitizer. Accordingly, further experiments were conducted in MeCN/H_2O 1:1 containing 50 mM phosphate buffer (pH 7) at a light intensity of 100 mW cm^{-2} and in the presence of 1.5 mM of the respective PS.

Under the above-mentioned conditions, we have investigated the photocatalytic activities of **MC3** and functionalized WOC ***m*-CH_2NMe_2-MC3** using **PS1-3** as sensitizers in phosphate buffered MeCN/H_2O 1:1 (pH 7, Figures S8 and S9). These experiments showed that the catalytic activity of ***m*-CH_2NMe_2-MC3** in terms of TOFs, TONs, ϕ_{chem} and Φ is quite similar to **MC3** (Table 1). Hence, the catalytic efficiency of the functionalized Ru(bda) macrocycle is not considerably affected by the incorporated tertiary amino groups indicating that the intrinsic catalytic activities of macrocycles **MC3** and ***m*-CH_2NMe_2-MC3** are comparable. Since ***m*-CH_2NMe_2-MC3** is better soluble in aqueous mixtures, the catalytic activities of this WOC were further studied in 5% MeCN and the results are compared with those obtained in 50% MeCN for both WOCs (Table 1).

Catalyst concentration-dependent studies of photocatalytic activity of **MC3** in 50% acetonitrile revealed that the initial rates of catalysis (Figure 4a) as well as TOF and TON values of the WOC, ϕ_{chem} and Φ are strongly dependent on the choice of photosensitizer (Table 1, Figure S8). The highest catalytic activity of **MC3** was obtained with the standard sensitizer **PS1** (TOF = 10.9 s^{-1}, TON = 430), while with sensitizers **PS2** and **PS3** the TOFs decreased significantly to 2.8 s^{-1} and 0.5 s^{-1}, respectively. A similar trend was observed for Ru macrocycle ***m*-CH_2NMe_2-MC3** in the same solvent mixture (Figure S9). It should be noted that in all cases the initial rates of oxygen production plotted against the total amount of WOC follow a linear relationship. This is indicative of first order kinetics

Table 1. Catalytic activities of **MC3** and ***m*-CH_2NMe_2-MC3** in photochemical water oxidation with **PS1–3** as sensitizers at varying MeCN content.

Sensitizer	**MC3** in 50% MeCN[a]				***m*-CH_2NMe_2-MC3** in 50% MeCN[b]				***m*-CH_2NMe_2-MC3** in 5% MeCN[c]			
	TOF [s^{-1}]	TON	Φ [%][d]	ϕ_{chem} [%][e]	TOF [s^{-1}]	TON	Φ [%][d]	ϕ_{chem} [%][e]	TOF [s^{-1}]	TON	Φ [%][d]	ϕ_{chem} [%][e]
PS1	10.9	430	2.9	1.6	9.5	550	2.6	2.3	2.9	270	2.0	0.5
PS2	2.8	220	0.3	0.6	2.2	180	0.4	0.8	10.8	320	3.0	0.7
PS3	0.5	170	0.1	0.3	0.4	100	0.1	0.4	0.7	100	0.3	0.3

[a] Measurements in MeCN/H_2O 1:1 (50 mM phosphate buffer, pH 7), c(PS) = 1.5 mM, $c(Na_2S_2O_8)$ = 37 mM, c(**MC3**) = 60 nM–2.5 μM. [b] Measurements in MeCN/H_2O 1:1 (50 mM phosphate buffer, pH 7), c(PS) = 1.5 mM, $c(Na_2S_2O_8)$ = 37 mM, c(***m*-CH_2NMe_2-MC3**) = 60 nM–2.5 μM. [c] Measurements in MeCN/H_2O 5:95 (50 mM phosphate buffer, pH 7), c(PS) = 0.2 mM, $c(Na_2S_2O_8)$ = 37 mM, c(***m*-CH_2NMe_2-MC3**) = 60 nM–2.5 μM. [d] Quantum yield of O_2 production determined for c(WOC) = 290 nM. [e] Chemical yield of O_2 production determined for c(WOC) = 880 nM.

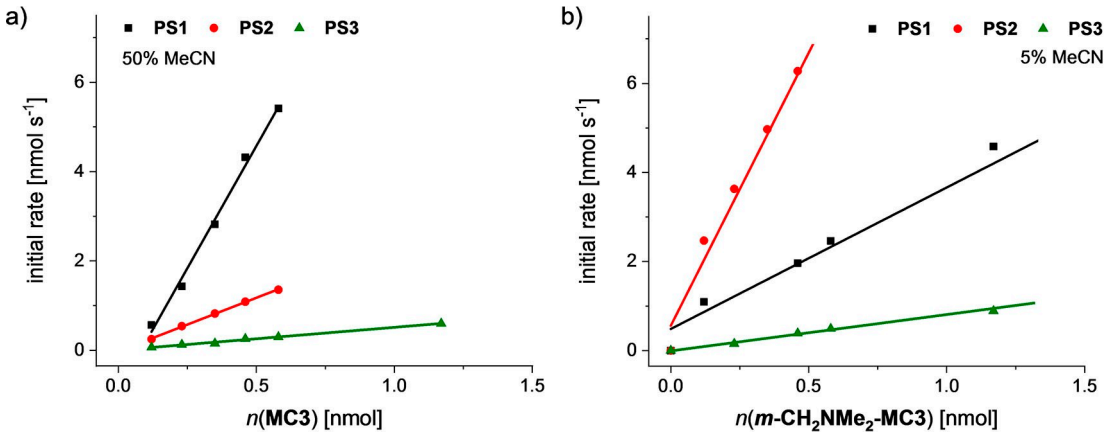

Figure 4. Catalytic performance of Ru(bda) macrocycles **MC3** (a) and ***m*-CH_2NMe_2-MC3** (b) in light-driven water oxidation using **PS1–3** as photosensitizers. The catalytic activity was analyzed by the initial rates of catalysis at variable WOC concentrations. Measurements were performed in (a) 1:1 or (b) 5:95 MeCN/H_2O mixtures (50 mM phosphate buffer, pH 7). Experiment conditions: (a) c(PS) = 1.5 mM, $c(Na_2S_2O_8)$ = 37 mM; (b) c(PS) = 0.2 mM, $c(Na_2S_2O_8)$ = 37 mM.

relative to the catalyst concentration and complies with the proposed WNA mechanism for WOC **MC3**.[19]

Interestingly, the trends in photocatalytic efficiency of ***m*-CH_2NMe_2-MC3** in combination with the present series of sensitizers are significantly different in 5% MeCN compared to 50% MeCN (Table 1, Figure S10). In 5:95 MeCN/H_2O mixture, WOC ***m*-CH_2NMe_2-MC3** reached the highest TOF of 10.8 s^{-1} with the ester-functionalized sensitizer **PS2**, whereas with the parent sensitizer **PS1** a modest TOF value of 2.9 s^{-1} was observed. It is noteworthy that due to lower solubility of the sensitizers in 5% MeCN, a reduced PS concentration had to be used in this solvent mixture to study the photocatalytic activity of ***m*-CH_2NMe_2-MC3**. For comparison, the photocatalytic activity of **MC3** was also measured at c(**PS2**) = 0.2 mM in 50% acetonitrile (Figure S11). In this case, TOF and TON of **MC3** decreased to 1.1 s^{-1} and 45 compared to 2.8 s^{-1} and 220 observed at c(**PS2**) = 1.5 mM. These results clearly underline the significance of sensitizer concentration for photocatalytic water oxidation with Ru macrocycles. Accordingly, the TOF (10.8 s^{-1}) and TON (320) values obtained for the ***m*-CH_2NMe_2-MC3/PS2** system with a 0.2 mM concentration of **PS2** in 5% acetonitrile are remarkably high. Catalytic samples of both Ru macrocycles **MC3** and ***m*-CH_2NMe_2-MC3** in MeCN:H_2O 1:1 and 5:95 were studied before and after catalysis by UV/Vis absorption spectroscopy (Figure S12). These experiments revealed a significant degradation of the photosensitizers in both solvent mixtures that presumably explains the end of catalysis under the studied reaction conditions. To assess any possible effect of the counter-ions of photosensitizers on photocatalytic efficiency, control experiments with macrocycle **MC3** in combination with **PS1** as hexafluorophosphate salt were performed in phosphate buffered (pH 7) MeCN/H_2O 1:1 (Figure S13). These experiments resulted in similar TOF (11.4 s^{-1}) and TON (390) values as those obtained using the chloride salt of **PS1** under identical conditions (TON = 10.9 s^{-1}; TON = 430), thus suggesting a negligible role of counter-ions on the photocatalytic efficiency of Ru macrocycles.

2.3. Emission Quenching Studies

To get insights into the WOC activation by PS^+, which is generated by the reaction of PS* with sodium persulfate ($Na_2S_2O_8$), we have explored the quenching efficiency of excited sensitizers by the electron acceptor sodium persulfate using Stern-Volmer analysis according to Equation (7):[12,34]

$$\frac{I_0}{I} = 1 + \tau_0 k_q\, c(S_2O_8{}^{2-}) \qquad (7)$$

where I_0 and I are the emission intensity in the absence and presence of quencher, respectively, τ_0 is the emission lifetime in

the absence of quencher, k_q the bimolecular rate constant of the quenching process and $c(S_2O_8^{2-})$ the concentration of persulfate quencher. Hereby, emission spectra of photosensitizers **PS1–3** were measured at different concentrations of sodium persulfate under inert conditions (see SI for experimental details). As exemplarily shown in Figure 5a for the emission quenching of parent sensitizer **PS1** in the presence of sodium persulfate in MeCN/H_2O 1:1 (see Figure S14 for emission quenching of sensitizers **PS1–3** in buffered solutions of MeCN/H_2O 1:1 and 5:95), a decrease in emission intensity was clearly observed upon increasing the concentration of the electron acceptor. The ratio of I_0/I plotted against the concentration of persulfate for all sensitizers in both solvent mixtures followed a linear relationship as indicated by the Stern-Volmer plots (Figures 5b and S15).

As shown in Table S3 for sensitizers **PS1–3**, the rate constants k_q of emission quenching obtained from Stern-Volmer analysis are strongly dependent on the solvent system. For example, a high rate constant k_q of $(1.8\pm0.3)\times10^9\ M^{-1}s^{-1}$ was observed for the quenching of **PS1** in MeCN/H_2O 5:95 while in MeCN/H_2O 1:1 k_q decreases by more than one order of magnitude to $(8.1\pm0.2)\times10^7\ M^{-1}s^{-1}$. The k_q value observed for **PS1** in MeCN/H_2O 5:95 is in excellent agreement with values reported in literature in water ($k_q = 9.8\times10^8$–$1.1\times10^9\ M^{-1}s^{-1}$)[12,27a, 35] and relates to a very fast, nearly diffusion controlled process. Also for **PS2**, k_q decreased by one order of magnitude upon increasing the MeCN content from 5% to 50% (Table S3). In contrast, such a solvent effect was not observed for the photosensitizer **PS3** bearing carboxylic acid groups as similar k_q values were obtained in both solvent mixtures. The relatively low quenching rates obtained for **PS3**, independent of the used MeCN content, point at an overall inefficient oxidative quenching of this photosensitizer by sodium persulfate.

2.4. Laser Flash Photolysis

We have then studied the electron-transfer processes between sensitizers **PS1** and **PS2** and Ru macrocycles **MC3** and ***m*-CH_2NMe_2-MC3** by nanosecond laser flash photolysis in 1:1 and 5:95 MeCN/H_2O mixtures (phosphate buffer, pH 7). Both photosensitizers were excited close or at their respective MLCT absorption maximum ($\lambda_{ex\ PS1} = 460$ nm, $\lambda_{ex\ PS2} = 482$ nm) and oxidized using an excess of sodium persulfate. The formation of PS^+ was detected as a ground state bleach of the ^{1}MLCT absorption band at 455 nm. In the absence of a Ru macrocycle, the amount of oxidized PS^+ in MeCN:H_2O 1:1 remains appreciably constant within the time window of the experiment (black curves in Figures 6a and S16a). In MeCN:H_2O 5:95, a slow bleach recovery over a few ms is observed (black curves in Figure S16b,c). In the presence of variable concentrations of Ru macrocycles **MC3** and ***m*-CH_2NMe_2-MC3**, changes in the ΔOD signal at 455 nm (bleaching recovery) indicate faster regeneration of the ground state of the sensitizers upon electron transfer from the catalyst to PS^+ (Figures 6a and S16). The residual negative absorption left upon recovery of the bleaching is consistent with oxidation of the macrocyclic WOC.[23,36] The rates of the observed ΔOD changes (k_{obs}) for sensitizers **PS1** and **PS2** in MeCN/H_2O 1:1 plotted against the concentration of catalyst **MC3** follow a linear relationship (Figure 6b). Under pseudo-first order conditions due to excess of the WOC over photogenerated PS^+, bimolecular rate constants for the respective electron-transfer processes were determined from the slope of the linear correlation.[8,13a, b] Thus, a k_{ET} constant of $(3.5\pm0.2)\times10^7\ M^{-1}s^{-1}$ was obtained for the **PS1**/**MC3** system, while a one order of magnitude larger value of $(3.3\pm0.1)\times10^8\ M^{-1}s^{-1}$ was observed for the electron transfer between **MC3** and **PS2**. This is in agreement with the larger thermodynamic driving force for the hole transfer process resulting from the introduction of electron withdrawing ester groups into **PS2** compared to **PS1**. For comparison, the electron transfer between ***m*-CH_2NMe_2-MC3** and photosensitizers **PS1** and **PS2** was studied in 50% MeCN as well (Figure S17). As

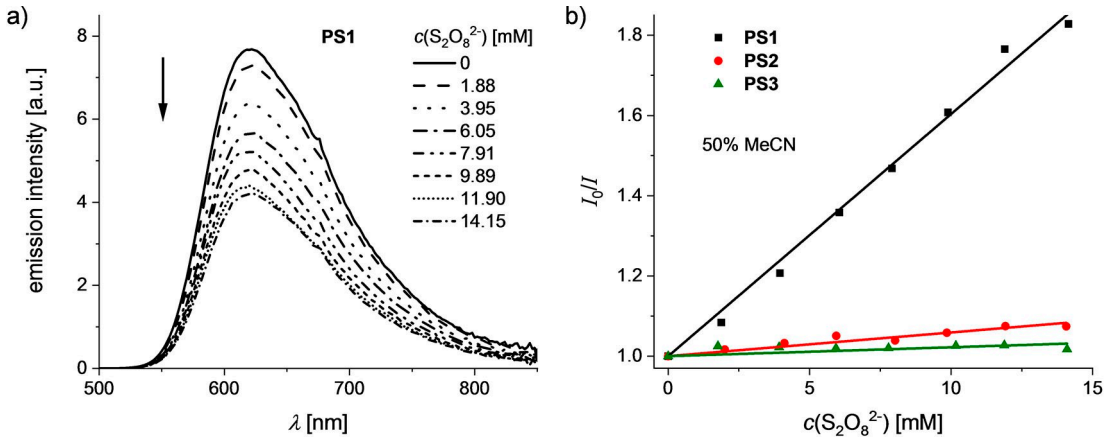

Figure 5. a) Emission spectra ($\lambda_{ex} = 453$ nm) of **PS1** in MeCN/H_2O 1:1 (phosphate buffer, pH 7) at varying concentrations of $Na_2S_2O_8$. The arrow indicates changes of emission spectra with increasing concentration of the persulfate quencher. b) Stern-Volmer plots showing linearly fitted curves for sensitizers **PS1–3** in buffered MeCN/H_2O 1:1 (pH 7). In all experiments, the concentration of the respective sensitizer was 50 μM.

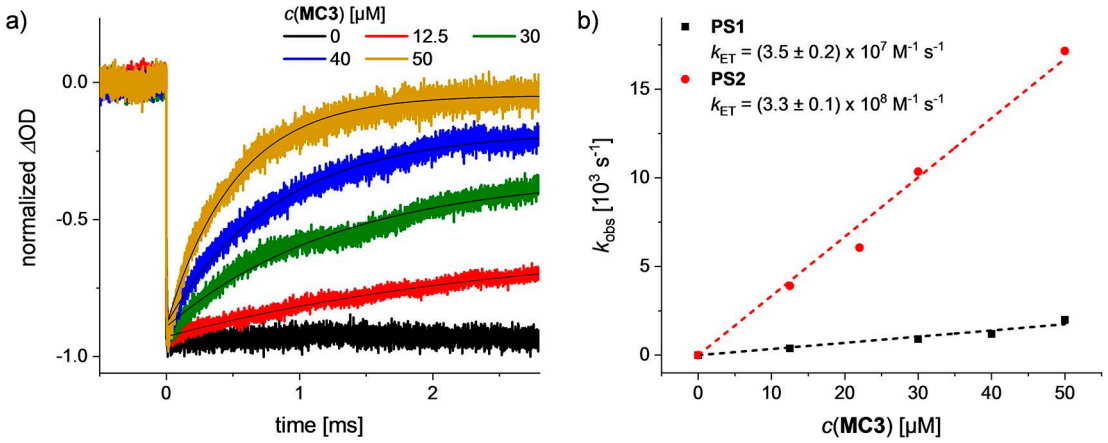

Figure 6. a) Kinetic traces at 455 nm of solutions of 50 μM **PS1** and 50 mM $Na_2S_2O_8$ in MeCN:H_2O 1:1 (50 mM phosphate buffer, pH 7) at variable concentrations of **MC3**. Exponential fits are shown in black. b) Plot of the observed rate constants k_{obs} for the electron transfer from **MC3** to oxidized sensitizers **PS1**$^+$ (black squares) and **PS2**$^+$ (red circles) *vs.* WOC concentration. k_{ET} is obtained from the slope of the linear correlation.

expected, k_{ET} values comparable to those determined for **MC3** were obtained. These rate constants are in line with those reported for mononuclear ruthenium catalysts.[8]

The electron-transfer processes between functionalized Ru macrocycle ***m*-CH_2NMe_2-MC3** and sensitizers **PS1** and **PS2** were then studied in 5% MeCN (Figure S16b,c). In this case, a bimolecular k_{ET} constant of $(7.3 \pm 0.6) \times 10^6$ M^{-1} s^{-1} was obtained for the electron transfer between the WOC and **PS2** (Figure S16d), a value almost two orders of magnitude lower than in 50% MeCN. Moreover, k_{ET} for the **PS1**/***m*-CH_2NMe_2-MC3** system can be estimated to be lower than 10^6 M^{-1} s^{-1} according to the low response observed in the catalyst concentration-dependent measurements shown in Figure S16c (exact determination is indeed hampered by experimental constraints, i.e. available time-window and WOC solubility). Considering the similar oxidation potentials of both sensitizers and macrocycles in the presence of different amounts MeCN,[23] the systematic reduction of k_{ET} values for ***m*-CH_2NMe_2-MC3** in 5% MeCN compared to 50% MeCN is probably related to the presence of the organic co-solvent and preferential solvation effects on the electron transfer kinetics. Notwithstanding, in both solvent mixtures a faster electron transfer from the WOC to the oxidized photosensitizers is always observed using **PS2** compared to **PS1**. Furthermore, these studies revealed a very strong dependency of the efficiency of electron transfer on the amount of organic co-solvent used.

3. Discussion

We have studied the photocatalytic activities of trinuclear Ru(bda) macrocycles **MC3** and ***m*-CH_2NMe_2-MC3** using a series of ruthenium tris(bipyridine) photosensitizers **PS1–3** in MeCN/H_2O mixtures containing varying amounts of MeCN as co-solvent to explore the effects of photosensitizers and co-solvent on catalytic efficiency of these WOCs. The experiments with **MC3** were performed in 50% MeCN, while studies with highly water-soluble ***m*-CH_2NMe_2-MC3** were conducted in 5% MeCN as well. The highest catalytic activity of Ru macrocycle **MC3** in 50% MeCN (TOF = 10.9 s^{-1}, TON = 430) was achieved with the standard ruthenium tris(bipyridine) sensitizer **PS1**. Similar catalytic activity (TOF = 9.5 s^{-1}, TON = 550) was observed for ***m*-CH_2NMe_2-MC3** with **PS1** under identical conditions. In contrast, in 5% MeCN ***m*-CH_2NMe_2-MC3** reached its best photocatalytic performance (TOF = 10.8 s^{-1}, TON = 320) with the carboxylic ester groups containing sensitizer **PS2**. It is noteworthy that due to the lower solubility of the sensitizers in 5% MeCN, a reduced PS concentration (c = 0.2 mM) had to be used to study the photocatalytic activity of ***m*-CH_2NMe_2-MC3** in this solvent mixture. In control experiments we could show the significance of sensitizer concentration for light-driven water oxidation with Ru macrocycles. Accordingly, the efficiency of the ***m*-CH_2NMe_2-MC3**/**PS2** system is remarkably high for the low sensitizer concentration in 5% MeCN. Further, it should be mentioned that both Ru macrocycles exhibit higher photocatalytic activities than most homogeneous Ru WOCs, including mononuclear Ru(bda) complexes that do not reach TOFs higher than 1 s^{-1}.[37] Importantly, a linear relationship between the catalyst amount and the initial rates of catalysis was observed for **MC3** and ***m*-CH_2NMe_2-MC3** in all photocatalytic water oxidation experiments. This complies with the first order kinetics of the proposed WNA mechanism of water oxidation for the unsubstituted WOC **MC3**.[19] Therefore, the diverse trends observed in photocatalytic efficiency of the Ru macrocycles with different photosensitizers cannot be ascribed to a change in operating mechanism of water oxidation, rather to the nature of the applied sensitizers and the solvent composition.

In photocatalytic water oxidation, the transfer of electrons to the sacrificial electron acceptor depends on the oxidation potentials of the components involved in the process and the resulting thermodynamic driving forces.[8] In Figure 7, a schematic energy diagram with relevant oxidation potentials is shown for photocatalytic water oxidation with WOC **MC3**, photosensitizers **PS1** and **PS2**, and sodium persulfate as sacrificial electron acceptor. In general, the higher is the

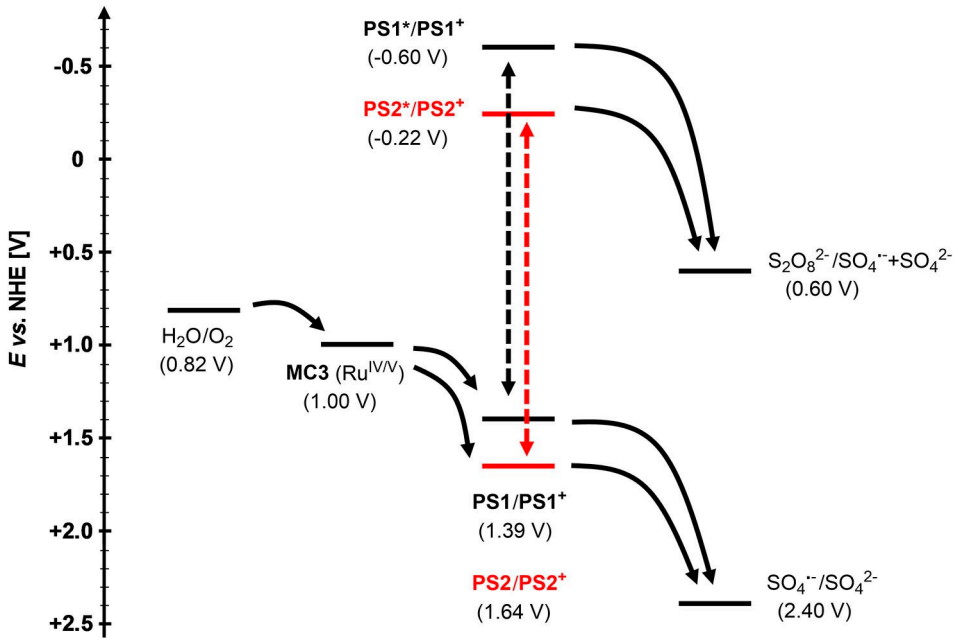

Figure 7. Energy scheme of photocatalytic water oxidation with **PS1** and **PS2** as photosensitizers, $Na_2S_2O_8$ as electron acceptor and trinuclear Ru(bda) macrocycle **MC3** as WOC (a similar situation applies for functionalized macrocycle ***m*-CH$_2$NMe$_2$-MC3**).[23] The potential for the oxidation of water to molecular oxygen at pH 7 was calculated by the Nernst equation: $E = 1.23 - (0.059 \times pH)$ V *vs.* NHE.[7,18] Oxidation potential of **MC3** was determined as described in Ref. [19]. Oxidation potentials of the sensitizers in ground and excited states were determined by cyclic voltammetry measurements and calculated as reported elsewhere,[8–9] respectively. Oxidation potentials of $Na_2S_2O_8$ according to Eqs. (2) and (3) in Figure 1 were obtained from literature references.[8,10–11]

potential at which the catalyst reaches its active state (e.g. 1.00 V for oxidation of **MC3** to Ru^{V} state at pH 7), the lower is the driving force for electron transfer from the WOC to the oxidized sensitizer. At the same time, replacing standard sensitizer **PS1** with **PS2** is expected to increase the driving force for the oxidation of **MC3** into its active state due to the higher Ru^{III}/Ru^{II} oxidation potential of the latter sensitizer as shown in Figure 7. Indeed, Sun and co-workers have reported that sensitizer **PS2** leads to higher TOF and TON values compared to **PS1** in photocatalytic water oxidation with a water soluble Ru(bda) WOC in pure water.[16b] However, we have observed the opposite behavior, i.e. higher TOF and TON values with **PS1** than **PS2** in light-driven water oxidation using Ru(bda) macrocycles **MC3** and ***m*-CH$_2$NMe$_2$-MC3** in MeCN/H_2O 1:1 mixture (Table 1). Nevertheless, considering the comparable excited state energy for both ruthenium dyes, changing of the sensitizer from **PS1** to **PS2** leads to a decrease in driving force for excited state oxidative quenching by the persulfate anion.

Photocatalytic water oxidation is usually dependent on the intrinsic catalytic ability of the WOC. However, the generation of the oxidized sensitizer PS^+ (by quenching of excited PS* by sodium persulfate) and the regeneration of ground state PS (by electron transfer from the WOC to PS^+) can also affect the efficiency of a photocatalytic system.[8,14b] Thus, the fact that **PS2** did not lead to an increase in TOF and TON compared to **PS1** in MeCN/H_2O 1:1 can be related to the electron transfer from the WOC to the oxidized sensitizers not being the rate-determining step of photocatalysis in this solvent mixture. Nanosecond flash photolysis was used to study the efficiency of this electron transfer in 50% MeCN revealing k_{ET} rate constants in the range of 10^7 to 10^8 M^{-1} s^{-1}. Notably, a one order of magnitude larger value was observed for the **PS2**/**MC3** system compared to **PS1** as expected due to introduction of electron withdrawing ester groups into sensitizer **PS2**. Stern-Volmer analysis was used to determine the rate constants of emission quenching for **PS1–3** in 50% MeCN. Interestingly, the obtained k_q values of 10^6–10^7 $M^{-1}s^{-1}$ relate very well to the trends observed for the photocatalytic activity of **MC3** with the series of functionalized sensitizers (**PS3** < **PS2** < **PS1**). Considering that these experiments were performed with same WOC of invariant intrinsic catalytic ability (i.e. the "dark" catalytic steps related to the WNA water oxidation mechanism of **MC3** are not rate-determining) we conclude that the photocatalytic performance of **MC3** in MeCN/H_2O 1:1 is most probably limited by the rate of generation of the respective photooxidant PS^+. This is also in agreement with the increase in TOF values observed upon increasing the light intensity up to 100 mW cm^{-2} which suggest the presence of a light-limiting kinetic regime as it has been recently observed for Ir WOCs in light-driven water oxidation using **PS1** as photosensitizer.[31,33] As a result, the different hole-transfer rates measured for the **PS1** and **PS2**/**MC3** systems did not considerably affect the efficiency of photocatalysis in 50% MeCN. The drastic decrease in TOF and TON values observed for the photosensitizer **PS3** can be explained by its inefficient quenching at pH 7 (in 50% MeCN and 5% as well) resulting from electrostatic repulsion between the negatively charged carboxylate groups of the sensitizer and the persulfate ions. This unfavorable situation might be avoided under strongly acidic conditions as suggested in a very recent publication by Concepcion and co-workers on the use of

phosphonate-functionalized ruthenium tris(bipyridine) derivatives as photosensitizers.[38]

Steady-state emission experiments further revealed that the quenching rates of excited photosensitizers **PS1*** and **PS2*** by sodium persulfate were significantly affected by the presence of the organic co-solvent. The respective k_q values were increased by one order of magnitude upon decreasing the content of MeCN from 50% to 5% (see Table S3). This effect may be related to a strong solvation of the sensitizers by the organic co-solvent in MeCN/H_2O mixtures which could hinder an efficient quenching at higher MeCN contents.[27a] We infer that the larger thermodynamic driving force resulting from use of **PS2** as photosensitizer compared to **PS1** becomes effective upon reduction of the MeCN content since the generation of photooxidant PS^+ in MeCN/H_2O 5:95 is very efficient. Thus, this explains the higher TOF and TON values obtained for the **PS2**/***m*-CH$_2$NMe$_2$-MC3** system in 5% MeCN compared to **PS1**. However, in this solvent mixture a significant reduction in k_{ET} values of about two orders of magnitude was observed for both **PS1** and **PS2** photosensitizers compared to the values obtained in 50% MeCN. Although in our experiments only the primary hole-transfer from the oxidized sensitizers to the Ru macrocycles in their Ru^{II} oxidation state is investigated, subsequent hole-transfer processes to the oxidized WOCs are likely to be affected in a similar way. Therefore, we conclude that in MeCN/H_2O 5:95 the overall photocatalytic efficiencies of the Ru macrocycles in terms of TOF and TON values is most likely limited by the hole-transfer process from photogenerated PS^+ to the WOC.

To the best of our knowledge, the direct influence of the organic co-solvent on the photocatalytic performance of homogeneous Ru WOCs has solely been studied in one recent publication by Sun and co-workers.[39] They have reported an increase in photocatalytic TON values of the monomeric Ru(bda)(pic)$_2$ and a related dimeric catalyst using **PS1** as sensitizer upon increasing the MeCN content from 20% to 60% in phosphate buffered MeCN/H_2O mixtures. This finding was explained by an increase in the driving force for water oxidation provided by the photooxidized **PS1$^+$** sensitizer in solvent mixture containing higher amount of MeCN. In contrast, we observed an opposite trend using **PS1** in combination with the **MC3** macrocycle under otherwise identical conditions ($TON_{50\%\ MeCN} = 80$, $TON_{5\%\ MeCN} = 270$ at c(**PS1**) = 0.2 mM). Further, our investigations on the photocatalytic performance of trinuclear Ru(bda) macrocycle ***m*-CH$_2$NMe$_2$-MC3** revealed that with sensitizer **PS2** higher TOF and TON values can be achieved by reduction of MeCN content from 50% to 5%. This higher photocatalytic activity observed for the supramolecular WOCs at lower MeCN content is reasonable considering the ability of acetonitrile to competitively bind to the Ru centers of the WOC designed for coordination of water molecules.[40] Indeed, we have previously demonstrated that upon increasing the MeCN content in MeCN/H_2O mixtures the catalytic efficiency of ***m*-CH$_2$NMe$_2$-MC3** and other trinuclear Ru(bda) macrocycles decreases in chemical water oxidation as well.[19,23]

On a more general basis, the present work highlights how in complex photochemical reactions such as light-driven water oxidation, the use of photosensitizers with high oxidation potentials might become a powerful tool to boost photocatalysis, but only provided that catalyst activation represents the rate-determining step.[13b,17c] In this respect, environmental factors such as use of organic co-solvents, solvent composition, type and concentration of buffer, etc. play a pivotal role and direct assessment of these experimental parameters is of high relevance for the application of PS/WOC couple towards efficient water oxidation catalysis.

4. Conclusions

We have elucidated the effects of photosensitizers and reaction media on the efficiency of photocatalytic water oxidation with trinuclear Ru(bda) macrocycles **MC3** and ***m*-CH$_2$NMe$_2$-MC3** using a series of ruthenium tris(bipyridine) photosensitizers and sodium persulfate as an electron acceptor. In addition, we have explored the kinetics of generation of photooxidant PS^+ and electron transfer from the trinuclear catalysts to the oxidized sensitizers to gain a deeper insight into the complex process of the photocatalytic water oxidation with Ru(bda) macrocycles.

In catalytic water oxidation with the present series of photosensitizers, we observed diverse trends for the catalytic performance of **MC3** and ***m*-CH$_2$NMe$_2$-MC3** in MeCN/H_2O containing 50% and 5% of the organic co-solvent, respectively. The photocatalytic activities of both Ru macrocycles were significantly dependent on the applied sensitizer and amount of organic co-solvent used. In 50% MeCN, the highest TOF and TON values were reached by WOC **MC3** with the parent sensitizer **PS1**. In contrast, in 5% MeCN catalyst ***m*-CH$_2$NMe$_2$-MC3** exhibited its highest catalytic activity in combination with ester-functionalized sensitizer **PS2**, presumably due to the larger thermodynamic driving force for the electron transfer between WOC and sensitizer resulting from the introduction of the electron withdrawing groups. This became important only upon reduction of the MeCN content since in 50% MeCN the quenching of **PS2** by sodium persulfate and hence the generation of **PS2$^+$** is inefficient when compared to parent compound **PS1**. As a result, an enhanced catalytic activity of functionalized macrocycle ***m*-CH$_2$NMe$_2$-MC3** was observed by using photosensitizer **PS2** upon decreasing the MeCN content from 50% to 5% which can also be related to the ability of MeCN to compete with water for binding sites of Ru WOCs. However, our studies revealed that the photocatalytic performance of the trinuclear Ru catalysts (in terms of TOFs and TONs) in either solvent mixture is not limited by their intrinsic catalytic abilities, which are related to the presence of preorganized water networks in their macrocyclic cavities, but rather by the efficiency of photogeneration of oxidant PS^+ and the ability of this species to act as an oxidizing agent to the WOCs. Therefore, we conclude that to increase the efficiency of Ru(bda) macrocycles in light-driven water oxidation the design of new photosensitizers would be required which are able to generate stable photooxidants in high yields in the presence

of a minimum amount of organic co-solvents. We envision that high-performance photocatalytic systems for water splitting desired for application in solar fuel devices might be accessible with fully water-soluble WOCs in combination with properly functionalized photosensitizers.

Experimental Section

All experimental details are provided in the Supporting Information.

Acknowledgements

This project has received funding from the European Research Council (ERC) under the European Union's Horizon 2020 Research and Innovation Program (grant agreement No. 787937). A.-L. M.-C. thanks the Fonds der Chemischen Industrie for a Kekulé fellowship. The authors also thank Maximilian Roth for synthetic support. Open access funding enabled and organized by Projekt DEAL

Conflict of Interest

The authors declare no conflict of interest.

Keywords: homogenous catalysis · photocatalysis · photosensitizers · ruthenium complexes · water oxidation

[1] a) P. D. Frischmann, K. Mahata, F. Würthner, *Chem. Soc. Rev.* **2013**, *42*, 1847–1870; b) S. Berardi, S. Drouet, L. Francàs, C. Gimbert-Suriñach, M. Guttentag, C. Richmond, T. Stoll, A. Llobet, *Chem. Soc. Rev.* **2014**, *43*, 7501–7519; c) B. Zhang, L. Sun, *Chem. Soc. Rev.* **2019**, *48*, 2216–2264.
[2] R. Matheu, P. Garrido-Barros, M. Gil-Sepulcre, M. Z. Ertem, X. Sala, C. Gimbert-Suriñach, A. Llobet, *Nat. Rev. Chem.* **2019**, *3*, 331–341.
[3] M. D. Kärkäs, O. Verho, E. V. Johnston, B. Åkermark, *Chem. Rev.* **2014**, *114*, 11863–12001.
[4] a) J. D. Blakemore, R. H. Crabtree, G. W. Brudvig, *Chem. Rev.* **2015**, *115*, 12974–13005; b) M. D. Kärkäs, B. Åkermark, *Dalton Trans.* **2016**, *45*, 14421–14461; c) R. Matheu, M. Z. Ertem, C. Gimbert-Suriñach, X. Sala, A. Llobet, *Chem. Rev.* **2019**, *119*, 3453–3471.
[5] B. Zhang, L. Sun, *J. Am. Chem. Soc.* **2019**, *141*, 5565–5580.
[6] a) L. Duan, F. Bozoglian, S. Mandal, B. Stewart, T. Privalov, A. Llobet, L. Sun, *Nat. Chem.* **2012**, *4*, 418–423; b) L. Duan, C. M. Araujo, M. S. G. Ahlquist, L. Sun, *Proc. Mont. Acad. Sci.* **2012**, *109*, 15584–15588.
[7] F. Puntoriero, A. Sartorel, M. Orlandi, G. La Ganga, S. Serroni, M. Bonchio, F. Scandola, S. Campagna, *Coord. Chem. Rev.* **2011**, *255*, 2594–2601.
[8] M. Natali, F. Nastasi, F. Puntoriero, A. Sartorel, *Eur. J. Inorg. Chem.* **2019**, *2019*, 2027–2039.
[9] a) F. Puntoriero, S. Serroni, G. La Ganga, A. Santoro, M. Galletta, F. Nastasi, E. La Mazza, A. M. Cancelliere, S. Campagna, *Eur. J. Inorg. Chem.* **2018**, *2018*, 3887–3899; b) S. Campagna, F. Puntoriero, F. Nastasi, G. Bergamini, V. Balzani, in *Photochemistry and Photophysics of Coordination Compounds I* (Eds.: V. Balzani, S. Campagna), Springer Berlin Heidelberg, Berlin, Heidelberg, **2007**, pp. 117–214.
[10] A. R. Parent, R. H. Crabtree, G. W. Brudvig, *Chem. Soc. Rev.* **2013**, *42*, 2247–2252.
[11] A. Harriman, G. Porter, P. Walters, *J. Chem. Soc. Faraday Trans. 1* **1983**, *79*, 1335–1350.
[12] A. Lewandowska-Andralojc, D. E. Polyansky, *J. Phys. Chem. A* **2013**, *117*, 10311–10319.
[13] a) A. Lewandowska-Andralojc, D. E. Polyansky, R. Zong, R. P. Thummel, E. Fujita, *Phys. Chem. Chem. Phys.* **2013**, *15*, 14058–14068; b) L. Francàs, R. Matheu, E. Pastor, A. Reynal, S. Berardi, X. Sala, A. Llobet, J. R. Durrant, *ACS Catal.* **2017**, *7*, 5142–5150; c) M. Natali, M. Orlandi, S. Berardi, S. Campagna, M. Bonchio, A. Sartorel, F. Scandola, *Inorg. Chem.* **2012**, *51*, 7324–7331.
[14] a) H.-C. Chen, D. G. H. Hetterscheid, R. M. Williams, J. I. van der Vlugt, J. N. H. Reek, A. M. Brouwer, *Energy Environ. Sci.* **2015**, *8*, 975–982; b) B. Limburg, E. Bouwman, S. Bonnet, *ACS Catal.* **2016**, *6*, 5273–5284.
[15] a) P. K. Ghosh, B. S. Brunschwig, M. Chou, C. Creutz, N. Sutin, *J. Am. Chem. Soc.* **1984**, *106*, 4772–4783; b) P. Comte, M. K. Nazeeruddin, F. P. Rotzinger, A. J. Frank, M. Grätzel, *J. Mol. Catal.* **1989**, *52*, 63–84; c) N. D. Morris, M. Suzuki, T. E. Mallouk, *J. Phys. Chem. A* **2004**, *108*, 9115–9119; d) R. Matheu, M. Z. Ertem, J. Benet-Buchholz, E. Coronado, V. S. Batista, X. Sala, A. Llobet, *J. Am. Chem. Soc.* **2015**, *137*, 10786–10795.
[16] a) M. Hara, C. C. Waraksa, J. T. Lean, B. A. Lewis, T. E. Mallouk, *J. Phys. Chem. A* **2000**, *104*, 5275–5280; b) L. Wang, L. Duan, L. Tong, L. Sun, *J. Catal.* **2013**, *306*, 129–132.
[17] a) Y. Xu, L. Duan, L. Tong, B. Åkermark, L. Sun, *Chem. Commun.* **2010**, *46*, 6506–6508; b) M. N. Kushner-Lenhoff, J. D. Blakemore, N. D. Schley, R. H. Crabtree, G. W. Brudvig, *Dalton Trans.* **2013**, *42*, 3617–3622; c) S. Berardi, L. Francàs, S. Neudeck, S. Maji, J. Benet-Buchholz, F. Meyer, A. Llobet, *ChemSusChem* **2015**, *8*, 3688–3696.
[18] M. D. Kärkäs, B. Åkermark, *Chem. Rec.* **2016**, *16*, 940–963.
[19] M. Schulze, V. Kunz, P. D. Frischmann, F. Würthner, *Nat. Chem.* **2016**, *8*, 576–583.
[20] V. Kunz, J. O. Lindner, M. Schulze, M. I. S. Röhr, D. Schmidt, R. Mitrić, F. Würthner, *Energy Environ. Sci.* **2017**, *10*, 2137–2153.
[21] N. Agmon, *Chem. Phys. Lett.* **1995**, *244*, 456–462.
[22] A.-L. Meza-Chincha, J. O. Lindner, D. Schindler, D. Schmidt, A.-M. Krause, M. I. S. Röhr, R. Mitrić, F. Würthner, *Chem. Sci.* **2020**, *11*, 7654–7664 ..
[23] V. Kunz, M. Schulze, D. Schmidt, F. Würthner, *ACS Energy Lett.* **2017**, *2*, 288–293.
[24] a) Y.-J. Hou, P.-H. Xie, B.-W. Zhang, Y. Cao, X.-R. Xiao, W.-B. Wang, *Inorg. Chem.* **1999**, *38*, 6320–6322; b) M. Zhou, G. P. Robertson, J. Roovers, *Inorg. Chem.* **2005**, *44*, 8317–8325; c) B. H. Farnum, J. J. Jou, G. J. Meyer, *Proc. Mont. Acad. Sci.* **2012**, *109*, 15628–15633; d) M. R. Norris, J. J. Concepcion, C. R. K. Glasson, Z. Fang, A. M. Lapides, D. L. Ashford, J. L. Templeton, T. J. Meyer, *Inorg. Chem.* **2013**, *52*, 12492–12501.
[25] a) V. Gutmann, G. Gritzner, K. Danksagmuller, *Inorg. Chim. Acta* **1976**, *17*, 81–86; b) D. Ajloo, B. Yoonesi, A. Soleymanpour, *Int. J. Electrochem. Sci.* **2010**, *5*, 459–477.
[26] A. Juris, V. Balzani, F. Barigelletti, S. Campagna, P. Belser, A. von Zelewsky, *Coord. Chem. Rev.* **1988**, *84*, 85–277.
[27] a) H. S. White, W. G. Becker, A. J. Bard, *J. Phys. Chem.* **1984**, *88*, 1840–1846; b) J. V. Caspar, T. J. Meyer, *J. Am. Chem. Soc.* **1983**, *105*, 5583–5590.
[28] D. R. Weinberg, C. J. Gagliardi, J. F. Hull, C. F. Murphy, C. A. Kent, B. C. Westlake, A. Paul, D. H. Ess, D. G. McCafferty, T. J. Meyer, *Chem. Rev.* **2012**, *112*, 4016–4093.
[29] N. Song, J. J. Concepcion, R. A. Binstead, J. A. Rudd, A. K. Vannucci, C. J. Dares, M. K. Coggins, T. J. Meyer, *Proc. Mont. Acad. Sci.* **2015**, *112*, 4935–4940.
[30] J. Blanco-Gálvez, S. Malato-Rodríguez, E. Delyannis, V. G. Belessiotis, S. C. Bhattacharya, S. Kumar, in *Solar Energy Conversion and Photoenergy Systems: Thermal Systems and Desalination Plants, Vol. III*, EOLSS Publications, **2010**, pp.186–226.
[31] A. Volpe, C. Tubaro, M. Natali, A. Sartorel, G. W. Brudvig, M. Bonchio, *Inorg. Chem.* **2019**, *58*, 16537–16545.
[32] a) A. Vaidyalingam, P. K. Dutta, *Anal. Chem.* **2000**, *72*, 5219–5224; b) S. G. Farina, W. Yuey, C. Ambrose, P. E. Hoggard, *Inorg. Chim. Acta* **1988**, *148*, 97–100; c) C. T. Lin, W. Boettcher, M. Chou, C. Creutz, N. Sutin, *J. Am. Chem. Soc.* **1976**, *98*, 6536–6544.
[33] A. Volpe, M. Natali, C. Graiff, A. Sartorel, C. Tubaro, M. Bonchio, *Dalton Trans.* **2020**, *49*, 2696–2705.
[34] a) O. Stern, M. Volmer, *Phys. Z.* **1919**, *20*, 183–188; b) P. Thordarson, *Chem. Soc. Rev.* **2011**, *40*, 1305–1323.
[35] A. Harriman, G. Porter, P. Walters, *J. Chem. Soc. Faraday Trans. 2* **1981**, *77*, 2373–2383.
[36] Due to the overlying absorption between the sensitizers and the Ru macrocycles, the excitation light is partially absorbed by the catalysts. Nevertheless, control experiments with Ru macrocycles **MC3** and ***m*-CH_2NMe_2-MC3** in MeCN/H_2O 1:1 and 5:95 revealed that in the absence

of photosensitizers no significant changes in ΔOD signal at 455 nm result from sample excitation at 460 nm or 482 nm (Figure S18).
[37] L.-X. Xue, T.-T. Meng, W. Yang, K.-Z. Wang, *J. Photochem. Photobiol. B* **2015**, *152*, 95–105.
[38] L. Wang, D. W. Shaffer, G. F. Manbeck, D. E. Polyansky, J. J. Concepcion, *ACS Catal.* **2020**, *10*, 580–585.
[39] F. Li, C. Xu, X. Wang, Y. Wang, J. Du, L. Sun, *Chin. J. Catal.* **2018**, *39*, 446–452.
[40] L. Wang, L. Duan, Y. Wang, M. S. G. Ahlquist, L. Sun, *Chem. Commun.* **2014**, *50*, 12947–12950.

Manuscript received: June 7, 2020
Revised manuscript received: July 31, 2020
Version of record online: August 25, 2020